

1 **Allelic expression analysis of Imprinted and X-linked genes from bulk**
2 **and single-cell transcriptomes**

3

4 Paolo Martini^{1,6§}, Gabriele Sales^{1§}, Linda Diamante², Valentina Perrera^{2,3}, Chiara Colantuono⁴, Sara
5 Riccardo⁴, Davide Cacchiarelli^{4,5}, Chiara Romualdi^{1*} and Graziano Martello^{1*}

6

7

8

9 **Affiliations:**

10 ¹ Department of Biology, University of Padova, Padua, Italy.

11 ² Department of Molecular Medicine, Medical School, University of Padova, Padua, Italy.

12 ³ International School for Advanced Studies (SISSA/ISAS), Trieste, 34136, Italy.

13 ⁴ Telethon Institute of Genetics and Medicine (TIGEM), Armenise/Harvard Laboratory of
14 Integrative Genomics, Pozzuoli, Italy

15 ⁵ Department of Translational Medicine, University of Naples “Federico II”, Naples, Italy

16 ⁶ Department of Molecular and Translational Medicine, University of Brescia, Brescia, Italy

17

18

19 *e-mail: chiara.romualdi@unipd.it; graziano.martello@unipd.it

20 § Authors contribute equally to the work

21 †Current address: International School for Advanced Studies (SISSA/ISAS), Trieste, 34136, Italy.

22 **Abstract**

23

24 Genomic imprinting and X chromosome inactivation (XCI) are two prototypical epigenetic
25 mechanisms whereby a set of genes is expressed mono-allelically in order to fine-tune their
26 expression levels. Defects in genomic imprinting have been observed in several
27 neurodevelopmental disorders, in a wide range of tumours and in induced pluripotent stem cells
28 (iPSCs). Single Nucleotide Variants (SNVs) are readily detectable by RNA-sequencing allowing
29 determination of whether imprinted or X-linked genes are aberrantly expressed from both alleles,
30 although standardised analysis methods are still missing. We have developed a tool, named
31 BrewerIX, that provides comprehensive information about the allelic expression of a large,
32 manually-curated set of imprinted and X-linked genes. BrewerIX does not require programming
33 skills, runs on a standard personal computer, and can analyze both bulk and single-cell
34 transcriptomes of human and mouse cells directly from raw sequencing data. BrewerIX confirmed
35 previous observations regarding the bi-allelic expression of some imprinted genes in naive
36 pluripotent cells and extended them to preimplantation embryos. BrewerIX identified also
37 misregulated imprinted genes in breast cancer cells and in human organoids and identified new
38 genes escaping XCI in human somatic cells. We believe BrewerIX will be useful for the study of
39 genomic imprinting and XCI during development and reprogramming, and for detecting aberrations
40 in cancer, iPSCs and organoids. Due to its ease of use to non-computational biologists, its
41 implementation could become standard practice during sample assessment, thus raising robustness
42 and reproducibility of future studies.

43 **Introduction**

44

45 Gene imprinting is used to control the dosage of a specific set of genes (imprinted genes) by
46 selectively silencing one of the two copies of the gene (either the maternal or the paternal allele). In
47 female cells, also the genes on the X chromosome are expressed mono-allelically thanks to a
48 random epigenetic silencing mechanism called X chromosome inactivation (XCI).

49 X-linked and imprinting diseases are the most common congenital human disorders because loss-
50 of-function mutations in the single expressed allele will not be buffered by the second silenced
51 allele¹. Imprinted genes were initially isolated as regulators of fetal growth and their aberrant
52 expression has been related to cancer²⁻⁴. For these reasons, analyzing the imprinting and XCI status
53 is crucial in many fields including cancer research, regenerative medicine and assisted reproductive
54 technology.

55 Correct imprinting information is used to evaluate the quality of human induced pluripotent stem
56 cells (iPSCs)^{5,6}, while reactivation of X chromosome is expected in both human and murine naive
57 pluripotent cells^{6,7}. Although iPSCs hold the promise for effective approaches in regenerative
58 medicine, disease modelling and drug screening (for review see Perrera and Martello⁶), their safety
59 is compromised by frequent genetic and epigenetic aberrations, such as Loss of Imprinting (LOI) or
60 a variable X chromosome status^{8-16,5}. Organoids are becoming the system of choice for the study of
61 tissue morphogenesis, cancer and infections¹⁷⁻²¹. However, little is known about their epigenetic
62 stability and, in the case of brain organoids which are commonly derived from PSCs¹⁹⁻²¹, it is not
63 known whether epigenetic aberrations found in PSCs^{5,6} might be inherited in the organoids.

64

65 Allelic expression can be determined by the presence of Single Nucleotide Variants (SNVs) in
66 RNA-sequencing (RNAseq) data. However, at the time of writing, no standardized pipelines for
67 analysis of allelic expression of Imprinted and X-linked genes have been developed. Existing
68 pipelines use different combinations of tools and rely on different parameters that were set to

69 analyze specific data and to address specific questions^{5,22,23}. Moreover, these pipelines need skilled
70 bioinformaticians to be run. A complete and easy to use tool, which does not require programming
71 skills, is still missing.

72

73 Motivated by this need, we built BrewerIX, an app available for macOS and Linux Systems that
74 looks for bi-allelic expression of experimentally validated imprinted genes (see Supplementary
75 Table 1 and 2 for a manually curated list of human and mouse genes) and genes on the sex
76 chromosomes. Bi-allelic expression of imprinted genes will indicate LOI. Bi-allelic expression of
77 X-linked genes may indicate reactivation of the X chromosome, as expected in the early embryo²⁴
78 or in naive pluripotent stem cells^{7,14,15,25}, X chromosome erosion, as observed after extensive culture
79 of pluripotent cells²⁶, or simply escape of single genes from the XCI mechanisms, as recently
80 documented in somatic cells^{27,28}.

81 **Results and Discussion**

82

83 Here we present BrewerIX a standardized approach for the analysis of imprinted and X-linked
84 genes. Differently from other tools, its implementation strategy allows the user i) to perform fast
85 and efficient analyses from raw data to the final plots on a standard desktop or laptop computer
86 without requiring any programming skills, ii) to have a comprehensive information of imprinted
87 and X linked genes taken from different databases that have been manually curated to avoid results
88 mis-interpretation, iii) to graphically visualize the results in an easy and intuitive way. All these
89 features will guarantee results reproducibility and transparency letting the field grow.

90

91 **General overview**

92 BrewerIX (freely available at <https://brewerix.bio.unipd.it>) is implemented as a native graphical
93 application for Linux and macOS. It takes as input either bulk or single-cell RNAseq data (fastq
94 files), analyzes reads mapped over the SNVs distributed on imprinted genes (see “Knowledge base”
95 section for details), X chromosome and Y chromosome and generates imprinting and XCI profiles
96 of each sample.

97 BrewerIX implements three pipelines with different aims (Fig. 1a, Supplementary Fig. 1). The
98 Standard pipeline is meant to rapidly have the imprinting and X inactivation status of a set of
99 samples (Fig. 1a). Here, BrewerIX will align each sample, filter alignments and call Allele Specific
100 Expression (ASE) Read counter (see sections below for technical details) using a set of pre-
101 compiled bi-allelic SNVs. Before visualization, SNVs are collapsed by genes to create a table that is
102 displayed by the user interface (UI). The Complete pipeline sacrifices speed for the sake of
103 completeness by using a larger set of SNVs (the bi-allelic set used in the Standard pipeline plus the
104 bi-allelic set called on the user dataset using a pre-compiled set of multi-allelic SNVs). The use of a
105 larger set of SNVs will increase the power to detect bi-allelic expression. The Tailored pipeline uses
106 a specific set of SNVs that the user might detect from whole genome or whole exome sequencing

107 data, allowing to evaluate imprinting and X-inactivation starting directly from the actual SNV
108 profile of the samples (Supplementary Fig. 1). While the input files for the Standard and the
109 Complete pipelines are only fastq files derived from RNAseq experiments, the Tailored pipeline
110 additionally requires the VCF file with a set of bi-allelic SNVs. To speed-up the analysis BrewerIX
111 allows multicore processing.

112

113 The end-point of the pipelines is a table (called "brewer-table") that is visualized by the UI. The UI
114 presents the results using two graphical panels. The gene summary panel shows a matrix of dots
115 with as many rows as the number of genes (ordered according to their genomic position) and as
116 many columns as the number of samples analyzed (position of the samples can be arranged just
117 dragging them in the desired order). The size and the colour of the dot are proportional to the
118 confidence of our estimate: i) the larger the dot, the higher the number of SNVs supporting our
119 estimate; ii) the brighter the colour, the closer to 1 is the average of the allelic ratios (minor/major)
120 of all bi-allelic SNVs. Empty dots are expressed genes with no evidence of bi-allelic expression.
121 Gray squares mean that the gene was detected but did not reach the user's thresholds, while the
122 absence of any symbol indicates that the gene was not detected (0 reads mapping on SNVs).

123 The SNVs summary panel shows a set of barplots (one set for each sample) with as many bars as
124 the number of SNVs per gene. Here blue is the colour of the reference allele and red is the
125 alternative/minor one. Solid colours indicate bi-allelic SNVs, transparent colours indicate mono-
126 allelic SNVs, while those SNVs that do not meet the minimum coverage are shown in gray. When a
127 gene shows no evidence of any genuine bi-allelic SNVs, we collapse the counts over a virtual SNV
128 (named "rs_multi") to give an indication of its expression.

129

130 The UI allows to set different filters: on SNVs and on genes. The filters on SNVs are based on the
131 following 4 parameters:

132 1. the overall depth (OD), representing the number of reads mapping on a given SNV;

- 133 2. the minor allele count (MAC), indicating the absolute number of reads mapping on the less
134 frequent SNV variant among the two detected (i.e. the minor allele);
- 135 3. the threshold to call a bi-allelic SNV, which can be either a cutoff on the allelic ratio (AR,
136 minor/major allele) or the p-value of a binomial test²⁹;
- 137 4. the minimal number of bi-allelic SNVs needed to call a bi-allelic gene, based on the assumption
138 that when a gene is expressed bi-allelically, multiple bi-allelic SNVs should be detected.

139 The filter on genes allows the user to choose the set of genes to display: all, only those detected (i.e.
140 those with a sufficient OD) or only those genes that are bi-allelic in at least one sample that was
141 analyzed. Additionally, the user can control the source of imprinted genes to be included in the
142 analysis: human and mouse have 4 sources that can be combined (see “Knowledge base”
143 paragraph) with the additional possibility to exclude placental and/or isoform-dependent genes.
144 Finally, the user can control the allelic ratio measure, as either minor allele / major allele, or minor
145 allele / total counts.

146 Both genes and SNVs summary panels can be saved as PDF files. Moreover, the gene summary
147 panel can be exported as a tab-delimited file to allow further analysis. All exports reflect the filters
148 chosen.

149

150 **Default Parameters setting**

151 Default values of the parameters have been empirically selected to minimize the number of false
152 positives. A false positive call is a SNV not present in the DNA, detected only at the RNA level due
153 to sequencing and caller errors.

154 To precisely estimate the rate of false positives (FDR) we generated Whole Exome Sequencing
155 (WES) data for human male BJ fibroblasts and for two iPS cells lines (HPD00 and HDP04¹⁵) and
156 identified SNVs on all autosomes of each cell line. We then analyzed with BrewerIX RNAseq data
157 from the 3 cell lines and estimated the fraction of SNVs detected from transcriptomic data but not
158 confirmed by WES using different thresholds. As shown in Fig. 1b, we obtained a mean FDR of

159 6.67% using an $AR \geq 0.2$ - as in⁵ and²⁴-, an $OD = 20$ reads and $MAC = 4$. Lowering such
160 parameters to $OD = 15$ and $MAC = 3$ did not increase significantly (7.64%) the FDR in all samples
161 tested (BJ prop test p-value 0.4587; HPD00 prop test p-value 0.1713; HPD04 prop test p-value
162 0.01829), while a further reduction significantly increased the FDR to 9.60% (BJ prop test p-value
163 0.1086; HPD00 prop test p-value 0.04211; HPD04 prop test p-value 4.582e-09).

164

165 To further evaluate the false positive calls we analyzed genes on sex chromosomes of male cells, of
166 whom only a single allele is present. Thus, we analyzed bulk RNAseq samples of 6 normal male BJ
167 fibroblasts from 3 published datasets (see Supplementary Table 3, describing all datasets used in
168 this study). We collected on sex chromosomes all the SNVs with an $OD \geq 5$ reads in at least one
169 sample.

170 As shown in Supplementary Fig. 2, the mean frequency distribution of false positive calls on the X
171 chromosome dropped to 3 every 10^5 SNVs analyzed, using an $OD = 15$ and $MAC = 3$. Importantly, no
172 bi-allelic SNVs were detected on the Y chromosome in any of the analyzed samples.

173 To gain further confidence in methods based on RNAseq data, we calculated the number of false
174 positive calls detected by SNP-array, a technique specifically developed and extensively used to
175 detect SNVs. We analyzed genomic DNA from BJ fibroblasts profiled with Affymetrix Mapping
176 250K Nsp SNP Array (GEO accession GSE72531), and we found that the number of false positives
177 detected was 100 times higher (2 every 10^3 evaluated SNVs, Supplementary Fig. 3) confirming that
178 RNAseq data is more accurate in detecting allelic imbalance.

179

180 Although the defined thresholds minimize false positives, we investigated their power of detecting
181 actual bi-allelic genes. For this reason, we analyzed RNAs-seq data from female human naive
182 iPSCs (HPD08 - GSM2988908), bearing two active X chromosomes^{15,21}. We detected 104 bi-allelic
183 genes on the entire X chromosome out of 382 detected genes.

184 We performed a similar analysis on all genes located on autosomes - obviously excluding imprinted
185 genes - in 3 different cell lines and found that on average 35.5% of the protein coding genes
186 detected were bi-allelic (BJ fibroblasts 33% - 1145/3471; HPD00 31.5% - 1281/4068 and HPD04
187 42% - 1805/4295).

188 Overall, we conclude that the chosen parameters allow detection of bi-allelic expression while
189 minimizing false positive calls.

190

191 Our default parameters for standard bulk RNAseq samples (>10M reads/sample) are 20, 4 and 0.2
192 for OD, MAC and AR respectively. Additionally, we call a gene bi-allelic when at least 2 bi-allelic
193 SNVs are detected, in order to filter out potential sequencing artifacts.

194

195 **Case Studies**

196 To test BrewerIX functionalities we analyzed very diverse datasets, including both bulk and single-
197 cell RNAseq, different organisms (human and mouse) and different biological systems (iPSCs,
198 cancer cells, early embryonic development and organoids).

199

200 **Human induced Pluripotent Stem cells (iPSCs)**

201 Reprogramming of human somatic cells to pluripotency has been associated with imprinting
202 abnormalities⁶, both in the case of conventional, or “primed”, iPSCs and in the case of naive
203 iPSCs^{5,8-10,15,30-32}.

204 We analyzed 10 isogenic bulk RNAseq samples, including 6 BJ fibroblast, 1 primed iPSC and 3
205 naive iPSC lines. We run the analysis both with Complete pipeline (Fig. 1c) and Standard pipeline
206 (Supplementary Fig. 4), obtaining highly comparable results. MEG3, H19 and MEG8 showed bi-
207 allelic expression specifically in naive iPSCs (Fig. 1c-d), as previously reported^{15,32}.

208 To experimentally validate these results and further demonstrate the accuracy of the default
209 parameters, we performed Sanger sequencing after PCR amplification of genomic DNA from 1

210 naive iPSC line and confirmed the presence of 12 randomly selected SNVs (Supplementary Table 4
211 and Fig. 1e), while bi-allelic expression of MEG3 was confirmed in 3 independent naive iPSC lines
212 (Fig. 1e). An additional dataset of human fibroblasts (HFF) and matching naïve iPSCs (HPD06¹⁵)
213 was analyzed with Standard pipeline, confirming bi-allelic expression of H19 and MEG3 only in
214 naive cells (Supplementary Fig. 5), as previously reported^{15,25,32}.

215

216 **Murine Embryonic Stem cells (mESCs)**

217 We analyze a dataset of murine Embryonic Stem cells (mESCs) expanded under different culture
218 conditions. Yagi and colleagues reported that expanding mESCs in 2i/L conditions resulted in LOI,
219 while mESCs in S/L conditions mostly retained correct imprinting³³. With BrewerIX we obtained
220 highly similar results for the imprinted genes analyzed by Yagi and colleagues (Fig. 1f) and
221 detected 5 additional bi-allelic transcripts. We conclude that BrewerIX detected LOI events in both
222 human and mouse naive pluripotent stem cells from bulk RNAseq data, in agreement with previous
223 analyses^{15,32,33}.

224

225 Next, we wanted to compare the performance of BrewerIX on matching bulk and single-cell
226 RNAseq data. Using bulk samples from mESCs cultured in 2i/L or S/L conditions³⁰, we identified
227 13 LOI events, with Ddc and Zfp264 showing LOI specifically in 2i/L and Pon2, Peg10, Dhcr7 and
228 Gab1 showing LOI only in S/L (Fig. 1g), and the remaining 7 shared between the two conditions.

229 We then analyzed single-cell data (384 cells from 2i/L and 288 from S/L) using 15, 3 and 0.2 for
230 OD, MAC and AR respectively, in order to account for the sequencing depth, lower than bulk
231 samples. We also considered a gene bi-allelically expressed when a single SNVs was found bi-
232 allelic in at least 20% of cells analyzed expressing such gene (Fig 2a). We observed that Impact and
233 Inpp5, which displayed multiple bi-allelic SNVs in bulk analysis (Fig. 1g) were found bi-allelic also
234 in a large fraction (>50%) of single cells analyzed (Fig. 2a). Several LOI events were detected only
235 in bulk samples, possibly because single-cell RNAseq detects preferentially the 3' end of

236 transcripts, limiting the number of SNVs detected. Despite such limitations, some bi-allelic genes
237 could be detected only by single-cell RNAseq (Ccdc40 and Plagl1), indicating that only single-cell
238 RNAseq allows the detection of LOI events occurring in a limited fraction of cells.

239

240 **Single-cell analysis of mouse preimplantation embryos**

241 Deng and colleagues analyzed the gene expression of single cells from oocyte to blastocyst stages
242 of mouse preimplantation development describing that in female embryos the paternal X
243 chromosome is transiently activated at the four-cell stage and subsequently silenced³⁴. BrewerIX
244 results were highly concordant with those generated with a custom pipeline by Deng and
245 colleagues, confirming the transient reactivation of the paternal X chromosome (Fig. 2b and
246 Supplementary Fig. 6). Next, we observed an expected mono-allelic expression of imprinted genes
247 (Fig. 2c and Supplementary Fig. 7), although 9 of them showed bi-allelic expression at several
248 stages of pre-implantation embryos. We analyzed two additional datasets^{35,36} of early mouse
249 embryos and confirmed bi-allelic expression of such genes in multiple samples from at least two
250 independent studies. Of note, the bi-allelic expression of Zim3 and Usp29 was detected up to the 4-
251 cell stage and could be attributed to a mix of maternal and zygotic mRNAs, each expressing a
252 different allele (Supplementary Fig. 8). Conversely, the remaining 7 imprinted genes were bi-allelic
253 at the blastocyst stage, indicating defective imprinted gene expression.

254

255 **Santoni et al. / Garieri et al. dataset - Single cell-analysis of human somatic cells**

256 Next, we analyzed a human somatic single-cell RNAseq dataset²³ and observed that 15 genes
257 showed bi-allelic expression in 20% of cells (Fig. 2d). Only 2 of these genes (ATP10A and TFPI2)
258 were also found bi-allelic by the authors of the original study²³. We extended the analysis to X-
259 linked genes and found that, out of 583 detected genes, 27 genes escaped XCI in at least two
260 individuals (Fig. 2e). Notably, 18 out of 27 were previously identified as escapees³⁷, while the

261 remaining 9 were identified by BrewerIX. We conclude that BrewerIX efficiently identifies LOI
262 and XCI escape events occurring in small fractions of somatic cells from single-cell transcriptomes.

263

264 **Single-cell analysis of breast cancer**

265 Different cancers, such as breast, kidney and lung, are characterized by frequent expression level
266 changes of imprinted genes, often accompanied by DNA methylation level changes in several
267 imprinted domains, such as PEG3³⁸. To test whether BrewerIX could detect LOI events in cancer
268 cells, we analyzed 515 single-cell samples and matching bulk samples from 11 breast cancer
269 patients³⁹. Analysis of bulk samples using the Complete pipeline identified only 5 genes, each
270 expressed bi-allelically in only one sample. In stark contrast, analysis of single-cell data identified 9
271 genes bi-allelic in the majority of breast cancer samples.

272 Such results indicate that single-cell analyses outperform bulk analyses in the case of heterogeneous
273 cancer samples and that imprinting abnormalities might be much more widespread in cancer cells
274 than currently thought.

275

276 **Brain organoids**

277 Human PSCs have been recently shown to have the capacity to self-organize into 3D structures
278 containing different parts of the brain^{19–21,40}. Such structures have been named cerebral organoids,
279 or “mini-brains”^{20,21}. Moreover, it is also possible to obtain more homogeneous structures such as
280 retina or cortical organoids^{19,40–42}.

281 We first analyzed single-cell transcriptomes from fetal neural cortex⁴² and observed bi-allelic
282 expression of several imprinted genes (Fig. 3a), some of which were previously reported to be bi-
283 allelic in the brain, such as PPP1R9A and NTM⁴³. We then analyzed transcriptome from mini-
284 brains and cortical organoids and observed that the same genes were found bi-allelic in multiple
285 independent samples (Fig. 3a-b). We conclude that brain organoids faithfully recapitulate the tissue-
286 specific regulation of imprinted genes observed in the brain. Notably, we also observed that some

287 genes that are known to be imprinted in the brain⁴², such as DLK1, SMOC1 and L3MBTL1, were
288 bi-allelically expressed in some organoids, indicating LOI events associated with organoid
289 formation. However, DKL1 and L3MBTL1 frequently show LOI in hPSCs, therefore such
290 aberrations might be inherited during neural differentiation, as previously reported⁵. Overall our
291 results indicate aberrant expression of some imprinted genes in organoids, including genes
292 associated with neurodevelopmental defects and cancer⁶.

293

294 **Conclusions**

295 The results obtained by BrewerIX on the selected case studies outcompeted published custom
296 pipelines confirming and extending published results, demonstrating the reliability and usefulness
297 of the tool. For the analysis of relatively homogeneous cell populations, such as pluripotent cells in
298 culture, we conclude that bulk RNAseq data allowed robust identification of LOI events.
299 Conversely, when heterogeneous populations of cells, such as cancer samples, are analyzed, only
300 single-cell measurements allowed to detect widespread events of LOI or XCI escape, indicating that
301 such phenomena might have been underestimated for technical limitations.

302 Previous studies reported bi-allelic expression of some imprinted genes in both human and mouse
303 naive pluripotent cells^{5,32,33} and interpreted it as aberrations induced by *in vitro* culture under
304 specific conditions. We confirmed such observations for both human and murine cells, the latter
305 showing bi-allelic expression of several genes regardless of the culture conditions used.
306 Interestingly, analysis of 3 independent pre-implantation embryo datasets showed bi-allelic
307 expression of multiple imprinted genes, some of which (H13, Impact, Dhcr7, Snx14, Igf2r and
308 Pon2) were also bi-allelic in mESCs. Of note, similar conclusions have been drawn by Santini and
309 colleagues³⁶, suggesting that bi-allelic expression of some imprinted genes is normally occurring in
310 naive pluripotent cells *in vivo* and *in vitro*.

311

312 However, it is important to point out that the identification of mono- or bi-allelic expression by
313 BrewerIX is dependent on the existence of at least one genomic SNV on the locus of interest and it
314 is limited to those genes that are actively transcribed in the analyzed samples. For these reasons, a
315 gene detected as not bi-allelic by the tool is not necessarily referable as mono-allelic, since the
316 absence of any evidence of bi-allelic expression might be due to a poor coverage, a negligible
317 expression of the gene or to the absence of detectable SNVs in the locus of interest. This limitation
318 particularly affects the analysis of mono- or bi-allelic expression in samples derived from inbred
319 mouse strains, where genomic SNVs are extremely rare.

320 Nevertheless, due to the ease of use of BrewerIX to non-computational biologists, we believe that
321 its implementation could become standard practice during the assessment of newly generated
322 pluripotent cells and organoids, as well as for the study of the molecular mechanisms underlying
323 genomic imprinting and XCI in different tissues and developmental stages, hopefully raising
324 robustness and reproducibility of future studies.

325 **Methods**

326

327 **Knowledge base**

328 The Knowledge base contains the species genome with the genome index (for hisat2), the bi-allelic
329 and the multi-allelic SNV file (ENSEMBL variants annotation version 98; INDELS and the SNVs
330 whose reference alleles differ from the reference genome were removed), the regions with the genes
331 of interest i.e. imprinted genes and genes on the sex chromosomes.

332 We manually curated a comprehensive set of imprinted genes from different sources. For human
333 and mouse imprinted genes, we collected the data from the Geneimprint database
334 (<http://geneimprint.com/>) and Otago database (<http://igc.otago.ac.nz/home.html>). We excluded all
335 genes labeled as “Predicted” or “Not Imprinted” and manually curated “Conflicting Data”. We
336 added human imprinted genes identified by Santoni and colleagues²³ and mouse imprinted genes
337 regulated by H3K27me3 in the early embryo, identified by Inoue and colleagues⁴⁴. We have also
338 labeled placental-specific and isoform-dependent imprinted genes within the curated gene list.
339 Placental-specific imprinted genes were identified combining information from the Otago database
340 and from two additional studies – ⁴⁵ for human imprinted genes and ⁴⁶ for mouse genes. For
341 isoform-specific genes, we referred to Geneimprint (category: “Isoform Dependent”) and Otago
342 databases. The manually curated gene lists are shown in Supplementary Tables 1 and 2.

343

344 **Front-end implementation**

345 The BrewerIX graphical interface is distributed as a native application for both Linux and macOS.
346 It is written in the Haskell programming language and makes use of the wxWidgets cross-platform
347 GUI library. Plots are generated using the Cairo library and its PDF output capabilities. The Linux
348 version of the application is packaged using the AppImage tool.

349

350 **Back-end implementation**

351 The computational pipeline is implemented in Python and is available as a Python package called
352 brewerix-cli at <https://github.com/Romualdi-Lab/brewerix-cli>. The pipeline performs the alignment,
353 allelic count and creation of the “brewer-table”. The pipeline can be run also using the command
354 line interface (CLI) implemented by brewerix-cli itself. The final output of the CLI is the “brewer-
355 table” that is parsed by the user interface to produce the BrewerIX visual outputs. The CLI has been
356 thought for advanced users willing to analyze their own set of genes or genomes of different
357 species. The minimum required inputs are the following: a genome (fasta format) and its index for
358 hisat2, genome dict (computed with GATK) and genome fasta index, a bed file indicating the
359 region of interest (i.e. imprinted genes and genes on the sex chromosomes), a set of bi-allelic SNVs
360 with reference alleles that must be present in the reference genome. In the following we report the
361 technical details on each analysis step.

362 **Alignments.** BrewerIX requires fastq files as input. The pipeline works with homogeneous library
363 layout i.e. all fastq files are either single- or paired-end. The fastq files are aligned to a reference
364 genome. The user can choose between Mouse GRCm38.p6 or human GRCh38.p13 genome.
365 Alignments are performed using hisat2 (version 2.1.0, default parameters) and filtered to keep only
366 reads laying on genes of interest. Aligned reads are further processed according to GATK best
367 practices, i.e. marking duplicates, splitting reads with N in the cigar and performing base quality
368 scores recalibration (such post processing steps are optional in brewerix-cli).

369 **SNV calling.** SNVs are called only at multi allelic SNVs using HaplotypeCaller from GATK v4.1.
370 Calls are performed as if all the samples have the same genotype, i.e. all in the same batch. The
371 reference and the most represented alternative allele are selected. We set the following parameters:
372 “--max-alternate-alleles 1 -stand-call-conf 1 --alleles multi_allele_vcf_file --dbsnp
373 multi_allele_vcf_file”.

374 **Allelic count.** Allelic count is performed using ASEReadCounter with default parameters from
375 GATK v4.1. This tool, given a set of loci and a bam file, allows computing the reads bearing the
376 reference and the alternative allele. Sample-specific results are collapsed into an ASER table.

377

378 **WES Library Preparation**

379 Genomic DNA was extracted from BJ fibroblasts and two iPS cell lines, HPD00 and HPD04
380 (cultivated as described in ¹⁵, two replicates for each cell line) and quantified using the Qubit 2.0
381 fluorimetric Assay (Thermo Fisher Scientific); sample integrity, based on the DIN (DNA integrity
382 number), was assessed using a Genomic DNA ScreenTape assay on TapeStation 4200 (Agilent
383 Technologies).

384 Libraries were prepared from 100 ng of total DNA using a WES service (Next Generation
385 Diagnostics srl) which included library preparation, target enrichment using the Agilent V7 probe
386 set, quality assessment and sequencing on a NovaSeq 6000 sequencing system using a paired-end,
387 300 cycle strategy (2x150) (Illumina Inc.).

388

389 **WES Analysis.** The raw data were analyzed by Next Generation Diagnostics srl Whole Exome
390 Sequencing pipeline (v1.0) which involves a cleaning step by UMI removal, quality filtering and
391 trimming, alignment to the reference genome, removal of duplicate reads and variant calling ⁴⁷⁻⁵⁰.
392 Variants were finally annotated by the Ensembl Variant Effect Predictor (VEP) tool⁵.

393 The final set of variants was refined applying hard-filter according to GATK best practices. In
394 detail, we used GATK VariantFiltration $QD < 2.0$, $FS > 60.0$, $MQ < 40.0$, $SOR > 4.0$,
395 $MQRankSum < -12.5$ and $ReadPosRankSum < -8.0$.

396

397 **False Discovery Rate.** From the BrewerIX ASER table obtained from the RNAseq data, we
398 extracted the SNVs with an $OD = 5$ reads and $MAC \geq 1$. Using this set of SNVs we computed ASE
399 from WES data. For each sample, we extracted the set of SNV covered by at least 5 reads in

400 RNAseq and in both WES replicates. False positives are defined as the number of BrewerIX bi-
401 allelic SNVs without an heterozygous call in at least one WES replicate. False positives were
402 computed at three thresholds: 20 - 4; 15 - 3 and 10 - 2 respectively for OD and MAC.

403

404 **Case Studies Data**

405 All RNAseq data but three were downloaded from GEO database using fastq-dump from sra-tools
406 version 2.8.2. The mouse ESCs, bulk and single-cell Cortical organoid datasets were downloaded
407 from Array Express via direct link. All datasets images were created using the BrewerIX-core
408 imprinted genes (i.e. genes curated from Geneimprint DB and Otago) unless stated otherwise.
409 Moreover, images were created showing only “significant” genes with default parameters i.e OD=
410 20, MAC= 4, AR \geq 0.2 and at least two bi-allelic SNV per gene in bulk data, while we considered
411 a gene bi-allelic when at least one SNV was found bi-allelic with OD= 15 and MAC= 3 in the case
412 of single-cell data. For the organoid dataset, we manually selected a list of 14 imprinted genes for
413 Fig. 3a-b, moreover in the case of droplet-based single-cell RNA-sequencing data we had to
414 consider the samples as pseudo-bulk, rather than single-cell datasets, because the detected SNVs
415 were too few, independently from the sequencing depth.

416 **BJ fibroblast dataset** - We collected BJ RNAseq data from 3 sources on the GEO database:
417 GSE110377 (BJ fibroblast GSM2988896; primed iPSC GSM2988902, naive iPSC GSM2988898,
418 GSM2988903, GSM2988904), GSE126397 (BJ fibroblasts GSM3597749 and GSM3597750) and
419 GSE63577 (BJ fibroblasts GSM1553088-GSM1553090). To deal with the heterogeneous reads
420 layout (single- and paired-end) of the sequencing data, we aligned each batch to the reference
421 human genome using hisat2, with default parameters. We use BrewerIX-cli to run the analysis
422 starting from the alignment files (bam). We used the Complete pipeline and loaded the “brewer-
423 table” on the visual interface to explore the results.

424 **HFF dataset** - HFF samples were downloaded from GSE93226 (GSM2448850-GSM2448852)
425 while reprogrammed iPSC from GSE110377 (GSM2988900). As for the BJ fibroblast dataset, we

426 computed single- and paired-end alignments separately (hisat2, default parameters) and then run
427 brewerix-cli with Standard pipeline. Panels summarizing the results have been generated with
428 BrewerIX user interface.

429 **Yagi et al. dataset - mouse ESCs -** Yagi dataset (GEO accession GSE84164; GSM2425488-
430 GSM2425495) was fully analyzed by BrewerIX with the Complete -pipeline.

431 **Kolodziejczyk et al. / Kim et al. dataset - mouse ESCs -** In this dataset, we analyzed mES cells
432 cultured in 2i/L or S/L downloaded from Array Express under the accession E-MTAB-2600. We
433 analyzed three bulk samples (one cultured in 2i/L and two in S/L) and 682 single-cell samples (384
434 cultured in 2i/L and 288 in S/L).

435 Both bulk and single-cell RNAseq datasets were analyzed using BrewerIX with Standard pipeline.
436 Bulk data visualization of the three samples was performed using BrewerIX user interface.

437 Single-cell RNAseq results were visualized using custom R code available at
438 github.com/Romualdi-Lab/. Results were summarized by the two categories: 2i/L and S/L. We
439 analyzed genes that are expressed in at least 10 cells in at least one category. We considered a gene
440 bi-allelically expressed when at least one SNV was found bi-allelic in at least 20% of cells analyzed
441 expressing such gene (other parameters remain default).

442 **Deng et al. dataset - oocyte to blastocyst -** Single-cell RNAseq dataset were downloaded from
443 GEO accession GSE45719 (GSM1112490-GSM1112581 and GSM1112603-GSM1278045; female
444 samples include GSM1112504-GSM1112514, GSM1112528-GSM1112539, GSM1112543-
445 GSM1112553, GSM1112626-GSM1112640, GSM1112656-GSM1112661, GSM1112696-
446 GSM1112697, GSM1112702-GSM1112705; male samples include GSM1112490-GSM1112503,
447 GSM1112515-GSM1112527, GSM1112540-GSM1112542, GSM1112554-GSM1112581,
448 GSM1112611-GSM1112625, GSM1112641-GSM1112653, GSM1112654-GSM1112655,
449 GSM1112662-GSM1112695, GSM1112698-GSM1112701, GSM1112706-GSM1112765; for
450 remaining samples no sex specification were available). Analysis has been carried out using

451 BrewerIX with Standard pipeline. The computed values were used for downstream custom analysis
452 (code can be found at <https://github.com/Romualdi-Lab/>).

453 For the X chromosome, we performed the analysis plotting the average of the allelic ratios in each
454 developmental stage for male and female samples. We used developmental stages where both male
455 and female samples were present. Thus, we considered 4 male, 6 female in middle 2-cell
456 (mid2cell); 4 male, 6 female for late 2-cell (late2cell); 3 male, 11 female for 4-cell (4cell); 27 male,
457 23 female for 16-cell (16cell); 28 male, 15 female for early blastocyst (earlyblast). To detect
458 paternal X chromosome reactivation, we inferred that the maternal allele was the most expressed
459 allele in the mid2cell stage. Using maternal and paternal alleles inferred from the mid2cell stage, we
460 computed the maternal/paternal ratio in all other stages. To evaluate the performance of BrewerIX
461 in detecting paternal X chromosome reactivation, we downloaded Deng's processed dataset from
462 the supplementary material of the manuscript³⁴. To avoid any bias, we analyzed genes shared by
463 Deng's processed dataset and BrewerIX generated data.

464 For imprinted genes, we plotted the Average Allelic Ratio (AAR) for each gene in each
465 developmental stage. We grouped the samples into the following 3 categories: Cleavage: early2cell,
466 mid2cell, late2cell, 4cell; Morula: 8cell, 16cell; Blastocyst: earlyblast, midblast, lateblast.

467 **Borensztein et al. dataset - oocyte to blastocyst** - We analyzed Xist-wt single-cell samples from
468 GSE80810 (GSM2371473-GSM2371585). We run BrewerIX with Complete pipeline. We consider
469 a gene bi-allelic when at least one SNV was found bi-allelic with OD= 15 and MAC= 3. We
470 grouped samples into the following 3 categories: Cleavage stage: 2-cell, 4-cell; Morula 8-cell, 16-
471 cell; Blastocyst 32-cell, 64-cell.

472 **Santini et al. dataset - Blastocyst-stage embryos** - We analyzed 8 samples of blastocyst-stage
473 embryos from GSE152106 (GSM4603204-GSM4603211). We run BrewerIX with Complete
474 pipeline. We considered a gene bi-allelic when at least one SNV was found bi-allelic with OD= 15
475 and MAC= 3.

476 **Santoni et al. / Garieri et al. dataset - human somatic cells** - We used available data from 772
477 human fibroblasts (we analyzed 229, 159, 192 and 192 for IND1, IND2, IND3 and IND4
478 respectively) and 48 lymphoblastoid (IND5) cells from 5 female individuals (GEO accession
479 GSE123028, GSM3493332-GSM3494151).

480 Single-cell RNAseq dataset was analyzed using BrewerIX with Standard pipeline. The single-cell
481 RNAseq visual reports were produced with custom R code available at
482 <https://github.com/Romualdi-Lab/>.

483 Results were summarized by individuals. We analyzed genes that are expressed in at least 10 cells
484 in at least four individuals. For this dataset, we included all human sources of imprinted genes, i.e.
485 genes curated from geneimprint DB, Otago and from Santoni and colleagues (see “Knowledge
486 base” paragraph for details). We considered a gene bi-allelically expressed when at least one SNV
487 was found bi-allelic in at least 20% of analyzed cells that express that gene (other parameters
488 remain default).

489 **Chung et al. dataset - Breast cancer** - Chung and colleagues³⁹ analyzed 11 patients representing
490 four subtypes of breast cancer (luminal A - BC01 and BC02, luminal B - BC03, HER2+ - BC04,
491 BC05 and BC06 or triple-negative breast cancer - TNBC – BC07-11). They obtained 515 single-
492 cell transcriptome profiles and 12 matched samples with bulk RNAseq from 11 patients (GEO
493 accession GSE75688 all the samples listed in GSE75688_final_sample_information.txt.gz; B03 has
494 both primary breast cancer and lymph node metastases). Bulk samples from the breast cancer
495 dataset were analyzed using BrewerIX with Complete pipeline. Visual inspection was performed
496 using BrewerIX. The single-cell RNAseq dataset was run using the Complete pipeline. The single-
497 cell RNAseq visual reports were produced with custom R code.

498 Patients were included in the analysis if a corresponding bulk sample was analyzed. The number of
499 cells analyzed for each patient are the following: BC01=22, BC02=53, BC03=33, BC03LN=53,
500 BC04=55, BC05=76, BC06=18, BC07LN=52, BC08=22, BC09=55, BC10=15 and BC11=11.

501 We analyzed genes that were expressed in at least 2 cells in at least one sample. We considered a
502 gene bi-allelically expressed when at least one SNV was found bi-allelic in at least 20% of analyzed
503 cells that express that gene (other parameters remain default). Code to reproduce the figure can be
504 found at <https://github.com/Romualdi-Lab/> as well.

505 **Camp et al. dataset - Human Cerebral Organoids** - In this study, Camp and colleagues analyzed
506 734 single-cell transcriptomes from human fetal neocortex or human cerebral organoids (GEO
507 accession GSE75140, GSM1957048-GSM1957493, GSM1957495, GSM1957497, GSM1957499,
508 GSM1957501, GSM1957503, GSM1957505, GSM1957507, GSM1957509, GSM1957511,
509 GSM1957513, GSM1957515, GSM1957518, GSM1957520, GSM1957522, GSM1957524,
510 GSM1957526-GSM1957814). We run the analysis using BrewerIX with Standard pipeline". The
511 single-cell RNAseq visual reports were produced with custom R code starting from the "brewer-
512 table". Single cells were summarized according to their annotation available from GEO: we
513 collapsed according to the tissue of origin ("Dissociated whole cerebral organoid"; "Fetal
514 neocortex" and "Microdissected cortical-like ventricle from cerebral organoid") and the stage (12
515 weeks post-conception - 12-wpc, 13 weeks post-conception 13-wpc, 33 days, 35 days, 37 days, 41
516 days, 53 days, 58 days, 65 days). The numbers of cell analyzed for each tissue stage combination
517 are the following: fetal_Neural_Cortex 12-wpc = 164, fetal_Neural_Cortex 13-wpc = 62,
518 Vent_ESC_H9 53-days = 96, Vent_iPSC_409B2 58-days = 79, MiniBrain_iPSC_409B2_33-days =
519 40, MiniBrain_iPSC_409B2 35-days = 68, MiniBrain_iPSC_409B2 37-days = 71,
520 MiniBrain_iPSC_409B2 41-days = 74, MiniBrain_iPSC_409B2 65-days = 80. We analyzed genes
521 that were expressed in at least 10 cells in at least one category. We considered a gene bi-allelically
522 expressed when at least one SNV was found bi-allelic in at least 20% of analyzed cells expressing
523 that gene (other parameters remain default for single-cell data).

524 **Giandomenico et al. dataset - MiniBrains** - Giandomenico and colleagues profiled three neural
525 organoids derived from H9 and H1 (2) iPSC using 10Xv2 (GEO accession GSE124174).
526 Sequencing data were used as bulk samples, i.e. not dividing in single cells, because the detected

527 SNVs were too few, independently from the sequencing depth. We selected one run per organoids
528 to avoid any depth biases (SRA run ids SRR8368415, SRR8368423 and SRR8368431). The
529 analysis was run using BrewerIX with Complete pipeline, with default parameters.

530 **Quadrato et al. dataset - MiniBrains** - In this study, the authors profiled organoids at six and three
531 month age using single-cell sequencing (DropSeq; GSE accession GSE86153). Sequencing data
532 were used as bulk samples, i.e. not dividing in single cells, because the detected SNVs were too
533 few, independently from the sequencing depth. We selected one run per organoids to avoid any
534 depth biases (SRA run ids SRR4082002 and SRR4082026). The analysis was run using BrewerIX
535 with Complete pipeline, with default parameters.

536 **Pasca et al. dataset - Cortical Organoid** - Pasca and colleagues analyzed the expression of
537 Cortical Organoids (GEO accession GSE112137). We analyze 4 samples (bulk RNAseq) from 4
538 control cortical organoids (GSM3058370, GSM3058382, GSM3058394 and GSM3058406). The
539 analysis was run using BrewerIX with Complete pipeline, with default parameters.

540 **Lopez-Tobon et al. dataset - Cortical Organoid** - In this study, the author profiled cortical
541 organoids both in bulk (Array Express accession E-MTAB-8325) and single-cell RNAseq (10Xv2 -
542 Array Express accession E-MTAB-8337). We analyzed single-cell experiments as bulk samples, i.e.
543 not dividing in single cells, because the detected SNVs were too few, independently from the
544 sequencing depth. Overall we analyzed 3 cortical organoids derived from ESC (HUES8, bulk at 50
545 and 100 days - Array Express run ids ERR4198631 and ERR4198637; single-cell at 100 days -
546 Array Express run id ERR4229837) and 3 cortical organoids derived from iPSC (MIF3, bulk at 50
547 and 100 days - Array Express run id ERR4198633 and ERR4198639; single-cell at 50 days - Array
548 Express run id ERR4229861). We run bulk and single-cell RNAseq separately using BrewerIX with
549 default parameters.

550

551

552

553 **SNP detection via PCR followed by Sanger sequencing**

554 Genomic DNA (gDNA) was extracted from cellular pellets with Puregene Core Kit A (Qiagen)
555 according to the manufacturer's protocol; 1µg gDNA was used as a template for PCR using the
556 Phusion High-Fidelity DNA polymerase (NEB, cat. M0530L).

557 Total RNA was isolated from cellular pellets using a Total RNA Purification kit (Norgen Biotek,
558 cat. 37500), and complementary DNA (cDNA) was generated using M-MLV Reverse Transcriptase
559 (Invitrogen, cat. 28025-013) and dN6 primers (Invitrogen) from 1000 ng of total RNA following
560 the protocols provided by the manufacturers, including a step of TurboDNase treatment (Thermo
561 Scientific). cDNA was diluted 1:5 in water and used as a template for PCR using the Phusion High-
562 Fidelity DNA polymerase; gDNA and cDNA were amplified by PCR using primers detailed in the
563 Supplementary Table 5. PCR was conducted with the following program: denaturation at 98°C for
564 30s; 35 cycles of denaturation at 98°C for 10 s, annealing at a temperature depending on primer
565 sequence ($T_m - 5^\circ\text{C}$) for 30 s, elongation at 72°C for 15 s; final elongation at 72°C for 10 min.

566 PCR reaction products were resolved and imaged by agarose gel electrophoresis. The remaining
567 PCR products were purified using the QIAquickPCR purification kit (Qiagen, cat. 28106) and direct
568 sequencing was performed using the same primers used for PCR amplification. Each PCR region of
569 interest was sequenced at least twice, using both forward and reverse primers. Sanger sequencing
570 was performed by Eurofins Genomics (<https://www.eurofinsgenomics.eu/en/custom-dna-sequencing/gatc-services/lightrun-tube/>). Sequence analysis and peak detection were performed
572 using freely available ApE software (<https://jorgensen.biology.utah.edu/wayned/apex/>).

573

574 **Data Availability**

575 BrewerIX is freely available for academic users at <https://brewerix.bio.unipd.it> and all code and
576 tutorials are available at <https://github.com/Romualdi-Lab/brewerix-cli> under AGPL3 license.

577 All RNAseq data used in this study were publicly available and obtained from either the Gene
578 Expression Omnibus (GEO) database under the accession codes GSE110377, GSE126397,
579 GSE63577, GSE93226, GSE84164, GSE123028, GSE45719, GSE75688, GSE75140, GSE124174,
580 GSE86153, GSE112137, GSE80810 and GSE152106 or from Array Express under the accession
581 codes E-MTAB-2600 and E-MTAB-8325. Whole exome sequencing data generated in the current
582 study are available via the Sequence Read Archive (SRA) repository with BioProject ID
583 PRJNA705070.

584 Additional details about all datasets used in the study are in Supplementary Table 3. The raw
585 Sanger sequencing data file underlying Fig. 1e and Supplementary Table 4 are provided as a Source
586 Data file.

587 **References**

588

589 1. Monk, D., Mackay, D. J. G., Eggermann, T., Maher, E. R. & Riccio, A. Genomic imprinting
590 disorders: lessons on how genome, epigenome and environment interact. *Nat. Rev. Genet.* **20**,
591 235–248 (2019).

592 2. Peters, J. The role of genomic imprinting in biology and disease: an expanding view. *Nat.*
593 *Rev. Genet.* **15**, 517–530 (2014).

594 3. Kalish, J. M., Jiang, C. & Bartolomei, M. S. Epigenetics and imprinting in human disease.
595 *Int. J. Dev. Biol.* **58**, 291–298 (2014).

596 4. Goovaerts, T. *et al.* A comprehensive overview of genomic imprinting in breast and its
597 deregulation in cancer. *Nat. Commun.* **9**, 1–14 (2018).

598 5. Bar, S., Schachter, M., Eldar-Geva, T. & Benvenisty, N. Large-Scale Analysis of Loss of
599 Imprinting in Human Pluripotent Stem Cells. *Cell Rep.* **19**, 957–968 (2017).

600 6. Perrera, V. & Martello, G. How Does Reprogramming to Pluripotency Affect Genomic
601 Imprinting? *Front. Cell Dev. Biol.* **7**, (2019).

602 7. Sahakyan, A. *et al.* Human Naive Pluripotent Stem Cells Model X Chromosome
603 Dampening and X Inactivation. *Cell Stem Cell* **20**, 87–101 (2017).

604 8. Hiura, H. *et al.* Stability of genomic imprinting in human induced pluripotent stem cells.
605 *BMC Genet.* **14**, 32 (2013).

606 9. Johannesson, B. *et al.* Comparable Frequencies of Coding Mutations and Loss of Imprinting
607 in Human Pluripotent Cells Derived by Nuclear Transfer and Defined Factors. *Cell Stem Cell*
608 **15**, 634–642 (2014).

609 10. Ma, H. *et al.* Abnormalities in human pluripotent cells due to reprogramming mechanisms.
610 *Nature* **511**, 177–183 (2014).

611 11. Tchieu, J. *et al.* Female Human iPSCs Retain an Inactive X Chromosome. *Cell Stem Cell* **7**,
612 329–342 (2010).

- 613 12. Anguera, M. C. *et al.* Molecular Signatures of Human Induced Pluripotent Stem Cells
614 Highlight Sex Differences and Cancer Genes. *Cell Stem Cell* **11**, 75–90 (2012).
- 615 13. Kim, K.-Y. *et al.* X Chromosome of Female Cells Shows Dynamic Changes in Status during
616 Human Somatic Cell Reprogramming. *Stem Cell Rep.* **2**, 896–909 (2014).
- 617 14. Cantone, I. & Fisher, A. G. Human X chromosome inactivation and reactivation:
618 implications for cell reprogramming and disease. *Philos. Trans. R. Soc. B Biol. Sci.* **372**,
619 20160358 (2017).
- 620 15. Giulitti, S. *et al.* Direct generation of human naive induced pluripotent stem cells from
621 somatic cells in microfluidics. *Nat. Cell Biol.* **21**, 275–286 (2019).
- 622 16. Rugg-Gunn, P. J., Ferguson-Smith, A. C. & Pedersen, R. A. Epigenetic status of human
623 embryonic stem cells. *Nat. Genet.* **37**, 585–587 (2005).
- 624 17. Artegiani, B. & Clevers, H. Use and application of 3D-organoid technology. *Hum. Mol.*
625 *Genet.* **27**, R99–R107 (2018).
- 626 18. Sato, T. *et al.* Single Lgr5 stem cells build crypt-villus structures in vitro without a
627 mesenchymal niche. *Nature* **459**, 262–265 (2009).
- 628 19. Nakano, T. *et al.* Self-formation of optic cups and storable stratified neural retina from
629 human ESCs. *Cell Stem Cell* **10**, 771–785 (2012).
- 630 20. Lancaster, M. A. *et al.* Cerebral organoids model human brain development and
631 microcephaly. *Nature* **501**, 373–379 (2013).
- 632 21. Quadrato, G. *et al.* Cell diversity and network dynamics in photosensitive human brain
633 organoids. *Nature* **545**, 48–53 (2017).
- 634 22. Reinius, B. *et al.* Analysis of allelic expression patterns in clonal somatic cells by single-cell
635 RNA-seq. *Nat. Genet.* **48**, 1430–1435 (2016).
- 636 23. Santoni, F. A. *et al.* Detection of Imprinted Genes by Single-Cell Allele-Specific Gene
637 Expression. *Am. J. Hum. Genet.* **100**, 444–453 (2017).
- 638 24. Moreira de Mello, J. C., Fernandes, G. R., Vibranovski, M. D. & Pereira, L. V. Early X

- 639 chromosome inactivation during human preimplantation development revealed by single-cell
640 RNA-sequencing. *Sci. Rep.* **7**, 1–12 (2017).
- 641 25. Tomoda, K. *et al.* Derivation conditions impact x-inactivation status in female human
642 induced pluripotent stem cells. *Cell Stem Cell* **11**, 91–99 (2012).
- 643 26. Xie, P. *et al.* The dynamic changes of X chromosome inactivation during early culture of
644 human embryonic stem cells. *Stem Cell Res.* **17**, 84–92 (2016).
- 645 27. Cotton, A. M. *et al.* Analysis of expressed SNPs identifies variable extents of expression
646 from the human inactive X chromosome. *Genome Biol.* **14**, R122 (2013).
- 647 28. Tukiainen, T. *et al.* Landscape of X chromosome inactivation across human tissues. *Nature*
648 **550**, 244–248 (2017).
- 649 29. Patrat, C., Ouimette, J.-F. & Rougeulle, C. X chromosome inactivation in human
650 development. *Development* **147**, (2020).
- 651 30. Chang, G. *et al.* High-throughput sequencing reveals the disruption of methylation of
652 imprinted gene in induced pluripotent stem cells. *Cell Res.* **24**, 293–306 (2014).
- 653 31. Pólvara-Brandão, D. *et al.* Loss of hierarchical imprinting regulation at the Prader–
654 Willi/Angelman syndrome locus in human iPSCs. *Hum. Mol. Genet.* **27**, 3999–4011 (2018).
- 655 32. Pastor, W. A. *et al.* Naïve human pluripotent cells feature a methylation landscape devoid of
656 blastocyst or germline memory. *Cell Stem Cell* **18**, 323–329 (2016).
- 657 33. Yagi, M. *et al.* Derivation of ground-state female ES cells maintaining gamete-derived DNA
658 methylation. *Nature* **548**, 224–227 (2017).
- 659 34. Deng, Q., Ramsköld, D., Reinius, B. & Sandberg, R. Single-Cell RNA-Seq Reveals
660 Dynamic, Random Monoallelic Gene Expression in Mammalian Cells. *Science* **343**, 193–196
661 (2014).
- 662 35. Borensztein, M. *et al.* Xist -dependent imprinted X inactivation and the early developmental
663 consequences of its failure. *Nat. Struct. Mol. Biol.* **24**, 226–233 (2017).
- 664 36. Santini, L. *et al.* Novel imprints in mouse blastocysts are predominantly DNA methylation

- 665 independent. *bioRxiv* 2020.11.03.366948 (2020) doi:10.1101/2020.11.03.366948.
- 666 37. Garieri, M. *et al.* Extensive cellular heterogeneity of X inactivation revealed by single-cell
667 allele-specific expression in human fibroblasts. *Proc. Natl. Acad. Sci. U. S. A.* **115**, 13015–
668 13020 (2018).
- 669 38. Kim, J., Bretz, C. L. & Lee, S. Epigenetic instability of imprinted genes in human cancers.
670 *Nucleic Acids Res.* **43**, 10689–10699 (2015).
- 671 39. Chung, W. *et al.* Single-cell RNA-seq enables comprehensive tumour and immune cell
672 profiling in primary breast cancer. *Nat. Commun.* **8**, 1–12 (2017).
- 673 40. Watanabe, K. *et al.* Directed differentiation of telencephalic precursors from embryonic
674 stem cells. *Nat. Neurosci.* **8**, 288–296 (2005).
- 675 41. López-Tobón, A. *et al.* Human Cortical Organoids Expose a Differential Function of GSK3
676 on Cortical Neurogenesis. *Stem Cell Rep.* **13**, 847–861 (2019).
- 677 42. Camp, J. G. *et al.* Human cerebral organoids recapitulate gene expression programs of fetal
678 neocortex development. *Proc. Natl. Acad. Sci. U. S. A.* **112**, 15672–15677 (2015).
- 679 43. Babak, T. *et al.* Genetic conflict reflected in tissue-specific maps of genomic imprinting in
680 human and mouse. *Nat. Genet.* **47**, 544–549 (2015).
- 681 44. Inoue, A., Jiang, L., Lu, F., Suzuki, T. & Zhang, Y. Maternal H3K27me3 controls DNA
682 methylation-independent imprinting. *Nature* **547**, 419–424 (2017).
- 683 45. Okae, H. *et al.* Genome-Wide Analysis of DNA Methylation Dynamics during Early Human
684 Development. *PLOS Genet.* **10**, e1004868 (2014).
- 685 46. Okae, H. *et al.* Re-investigation and RNA sequencing-based identification of genes with
686 placenta-specific imprinted expression. *Hum. Mol. Genet.* **21**, 548–558 (2012).
- 687 47. Smith, T., Heger, A. & Sudbery, I. UMI-tools: modeling sequencing errors in Unique
688 Molecular Identifiers to improve quantification accuracy. *Genome Res.* **27**, 491–499 (2017).
- 689 48. Bolger, A. M., Lohse, M. & Usadel, B. Trimmomatic: a flexible trimmer for Illumina
690 sequence data. *Bioinforma. Oxf. Engl.* **30**, 2114–2120 (2014).

- 691 49. McLaren, W. *et al.* The Ensembl Variant Effect Predictor. *Genome Biol.* **17**, 122 (2016).
- 692 50. Freed, D., Aldana, R., Weber, J. A. & Edwards, J. S. *The Sentieon Genomics Tools - A fast*
- 693 *and accurate solution to variant calling from next-generation sequence data.*
- 694 <http://biorxiv.org/lookup/doi/10.1101/115717> (2017) doi:10.1101/115717.
- 695 51. Kolodziejczyk, A. A. *et al.* Single Cell RNA-Sequencing of Pluripotent States Unlocks
- 696 Modular Transcriptional Variation. *Cell Stem Cell* **17**, 471–485 (2015).

697 **Acknowledgements**

698 The authors thank members of the Martello laboratory for discussions and suggestions. G.M.'s
699 Laboratory is supported by grants from the Giovanni Armenise–Harvard Foundation, the Telethon
700 Foundation (TCP13013) and an ERC Starting Grant (MetEpiStem), C.R. is supported by the Italian
701 Association for Cancer Research (AIRC) [IG21837], P.M. has been supported by the European
702 Molecular Biology Organization (EMBO) Short-Term Fellowship [8517].

703

704 **Author contributions**

705 G.M., C.R. and P.M. designed the study; P.M. and G.S. developed the software and all custom
706 code; P.M. performed all analyses; V.P. and L.D. performed validation experiments; D.C. and C.C.
707 performed WES analyses. P.M. and L.D. prepared the figures; P.M., C.R. and G.M. wrote the
708 manuscript with input from all authors; G.M. and C.R. supervised the study and provided fundings.

709

710 **Competing interests**

711 The authors declare no competing interests.

712 **Figure Legends**

713

714 **Figure 1. Analyses of Imprinted gene expression in naive pluripotent cells with BrewerIX**

715 **a**, BrewerIX rational and overall implementation scheme for the Standard pipeline. **b**, False
716 discovery rate estimates obtained by comparing WES calls and BrewerIX bi-allelic calls in one
717 male BJ fibroblast and two iPSC cell lines. Three thresholds combination of overall depth (OD) and
718 minimal coverage of the minor allele (MAC) were used; True Positives (TP) in cyan; False
719 Positives (FP) in shades of orange. **c**, BrewerIX gene summary panel results on bulk RNAseq data
720 from isogenic human fibroblasts (BJ FIBRO), primed (HPD00) and naive (HPD01/3/4) iPSCs. The
721 larger the dot, the higher the number of SNVs supporting the bi-allelic call. The brighter the orange,
722 the closer to 1 is the average of the allelic ratios (minor/major) of all the bi-allelic SNVs. Empty
723 dots indicate detected genes with no evidence of bi-allelic expression, gray squares indicate genes
724 detected but not reaching the user's thresholds, while the absence of any symbol indicates that the
725 gene was not detected. **d**, BrewerIX SNV summary panel for MEG3 in the case study shown in
726 panel c. A barplot for each sample is reported, with as many bars as the number of SNVs per gene.
727 Solid colours represent actual SNV with both loci expressed, blue and red are the reference and the
728 alternative/minor allele. Transparent colours indicate SNVs detected with no evidence of bi-allelic
729 expression, while gray-scale colours indicate SNVs that do not meet the minimal coverage. **e**,
730 Experimental validation of the indicated MEG3 SNVs by PCR followed by Sanger sequencing. The
731 SNVs of interest are highlighted by a red box. See Supplementary Table 4 for a list of all SNVs
732 validated. Each SNVs was detected in two independent experiments, using either Forward or
733 Reverse sequencing primers. **f**, BrewerIX gene summary panel results on bulk RNAseq data
734 generated by Yagi and colleagues³³. Murine ESCs were expanded in either 2i/L or S/L conditions,
735 while mouse embryonic fibroblasts (MEF) serve as controls. **g**, BrewerIX gene summary panel
736 results from bulk RNAseq data of mESCs cultured in 2i/L or S/L (two biological replicates) by
737 Kolodziejczyk and colleagues⁵¹. See Fig. 2a for matching single-cell RNAseq samples.

738 **Figure 2. Analyses of single-cell RNAseq data of mouse embryonic and human adult cells**

739 **a**, Analysis of single-cell RNAseq data from mESCs cultured in 2i/L or S/L, matching those shown
740 in Fig. 1g. Results are summarised as percentages (degree of blue) of cells in which a given gene
741 was expressed bi-allelically. Number of cells analyzed: 2i/L 384, S/L 288. **b**, Average allelic ratio
742 (AAR) defined as the average of paternal/maternal ratios across single cells for all genes in X
743 chromosome in male and female embryonic cells detected by single-cell RNAseq³⁴. Wilcoxon tests
744 were performed between pairs of sequential developmental stages of female embryos (mid2cell -
745 late2cell, late2cell - 4cell, 4cell - 16cell, 16cell - earlyblast. Number of cells for male (M) and
746 female (F) for each developmental stage: mid2cell 6M, 6F; late2cell 4M, 6F; 4cell 3M, 11F; 16cell
747 27M, 23F; earlyblast 28M, 15F. See also Supplementary Fig. 6. **c**, Genes with frequent LOI across
748 mouse developmental stages obtained by studying three datasets³⁴⁻³⁶. On the y axis, the Average
749 Allelic Ratios (AAR) of single samples (single cells or single embryos for the Santini dataset).
750 Developmental stages have been collapsed into broader categories (Cleavage, Morula and
751 Blastocyst, see Methods). Number of cells for developmental stage: Deng et al. zygote 4, early2cell
752 8, mid2cell 12, late2cell 10, 4cell 14, 8cell 28, 16cell 50, earlyblast 43, midblast 60, lateblast 30;
753 Borensztein et al., 2-cell 6, 4-cell 10, 8-cell 29, 16-cell 15, 32-cell 26, 64-cell 20; Santini et al.
754 Blastocyst 8. See also Supplementary Fig. 7-8. **d**, Analysis of single-cell RNAseq data²³ from 772
755 human fibroblasts and 48 lymphoblastoid cells from 5 female individuals (IND1-5). Results are
756 summarised as percentages (degree of blue) of cells in which a given gene was expressed bi-
757 allelically. Gray indicates undetected genes. Number cells: IND1 229, IND2 159, IND3 192, IND4
758 192 and IND5 48. **e**, Results for X chromosome genes on samples described in panel d. **f**, BrewerIX
759 gene summary panel results from bulk RNAseq data from human breast cancer samples³⁹. LN
760 indicates matching metastatic lymph nodes. **g**, Analysis of single-cell RNAseq data from breast
761 cancer samples, matching those analyzed in panel f. Number of cells: BC01 22, BC02 53, BC03 33,
762 BC03LN 53, BC04 55, BC05 76, BC06 18, BC07LN 52, BC08 22, BC09 55, BC10 15, BC11 11.
763 Gray indicates undetected genes.

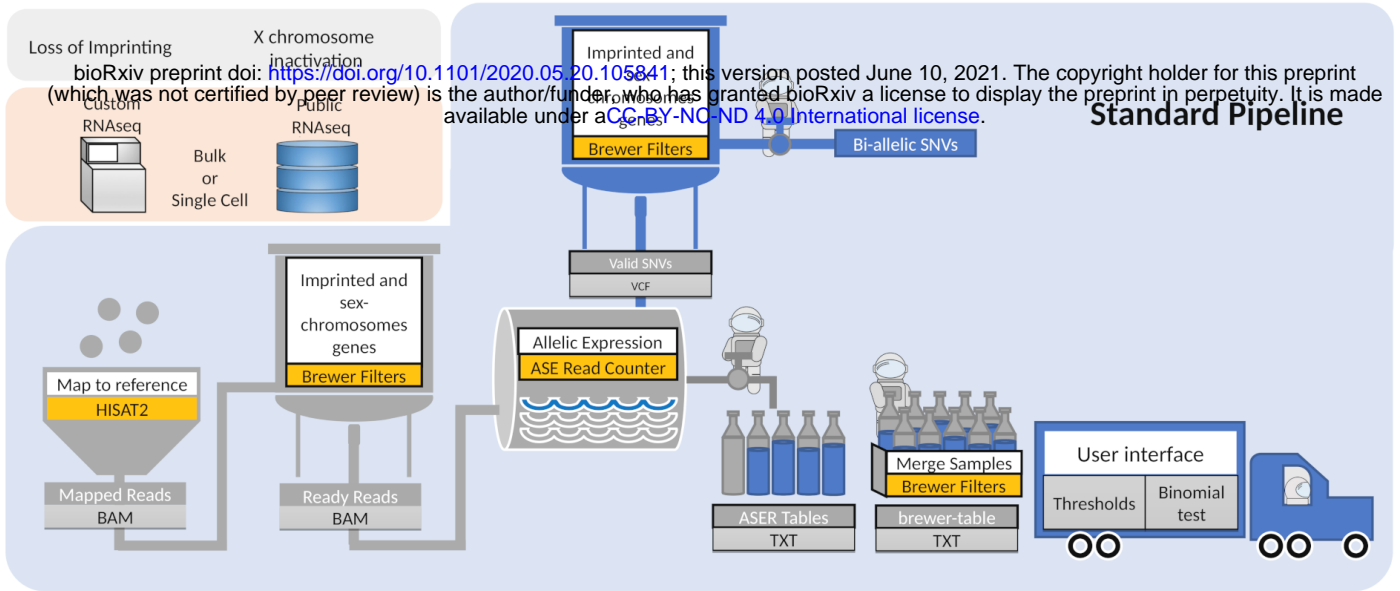
764 **Figure 3. Analysis of bulk and single-cell RNAseq data from human organoids for 14 selected**
765 **genes.**

766 **a**, Analysis of single-cell RNAseq data from fetal neocortex, cortical-like ventricle from cerebral
767 organoids (Vent) and whole cerebral organoids (minibrains). Gray indicates undetected genes. **b**
768 Summarized view of the imprinting status of 14 selected genes in 4 different studies in human
769 minibrains and cortical organoids.

FIGURE 1

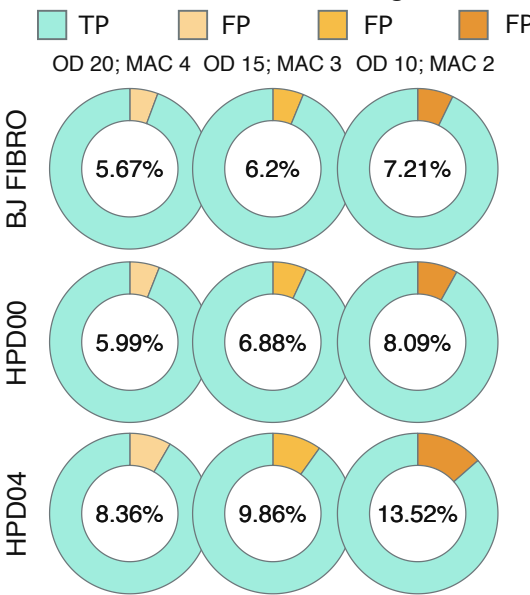
BrewerIX overview

a

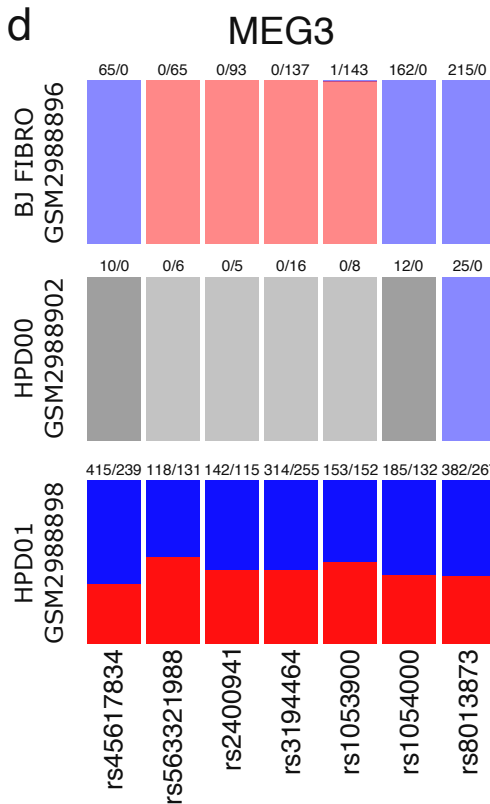


b

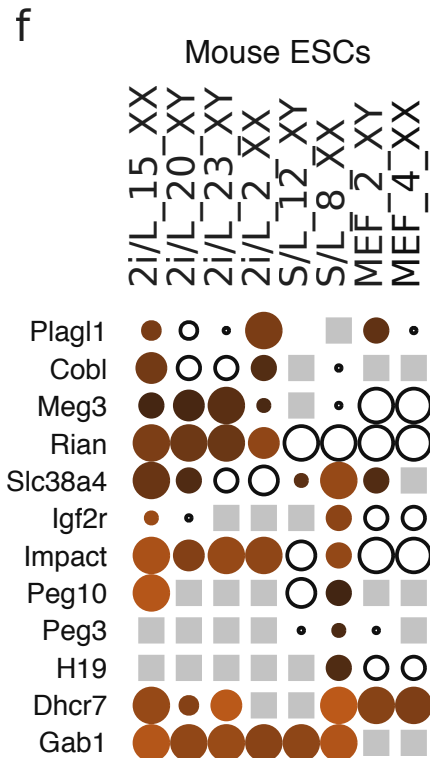
Parameters setting



d

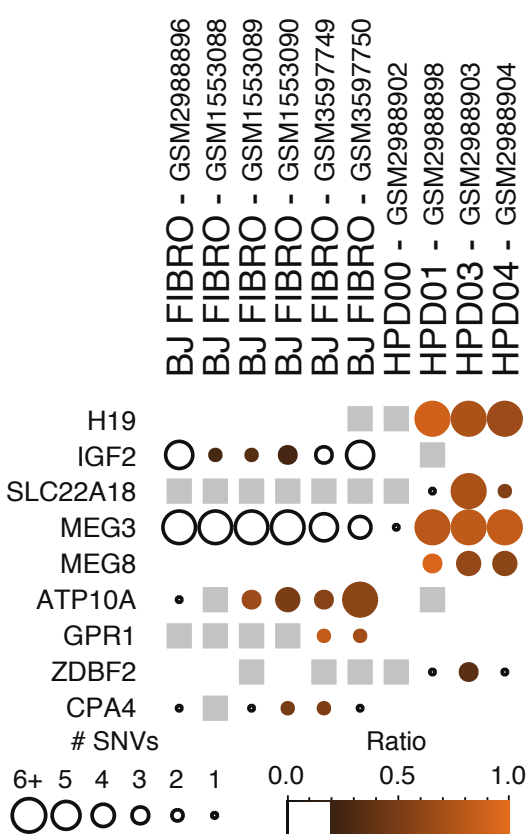


f

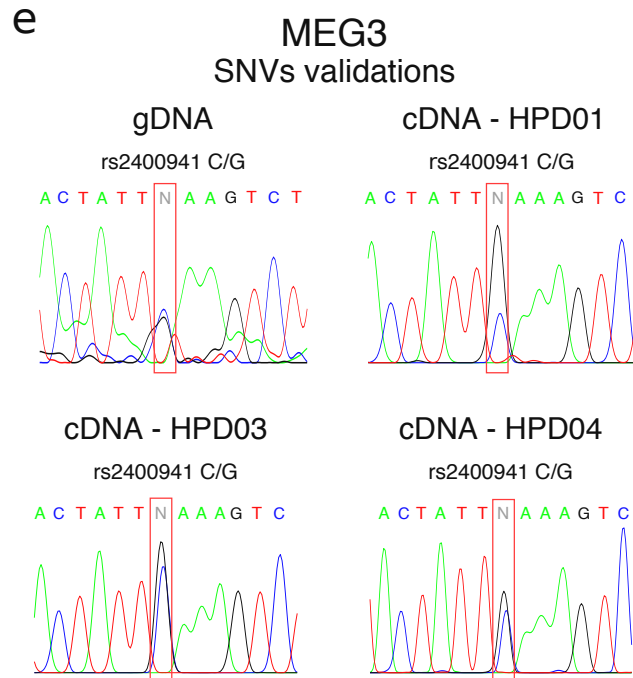


c

Reprogramming



e



g

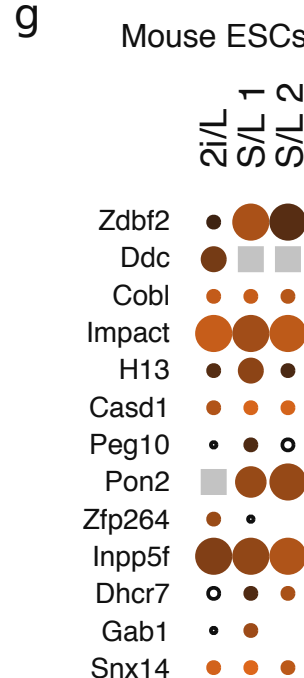


FIGURE 2

bioRxiv preprint doi: <https://doi.org/10.1101/2020.05.20.105841>; this version posted June 10, 2021. The copyright holder for this preprint (which was not certified by peer review) is the author/funder, who has granted bioRxiv a license to display the preprint in perpetuity. It is made available under a [CC-BY-NC-ND 4.0 International license](https://creativecommons.org/licenses/by-nc-nd/4.0/).

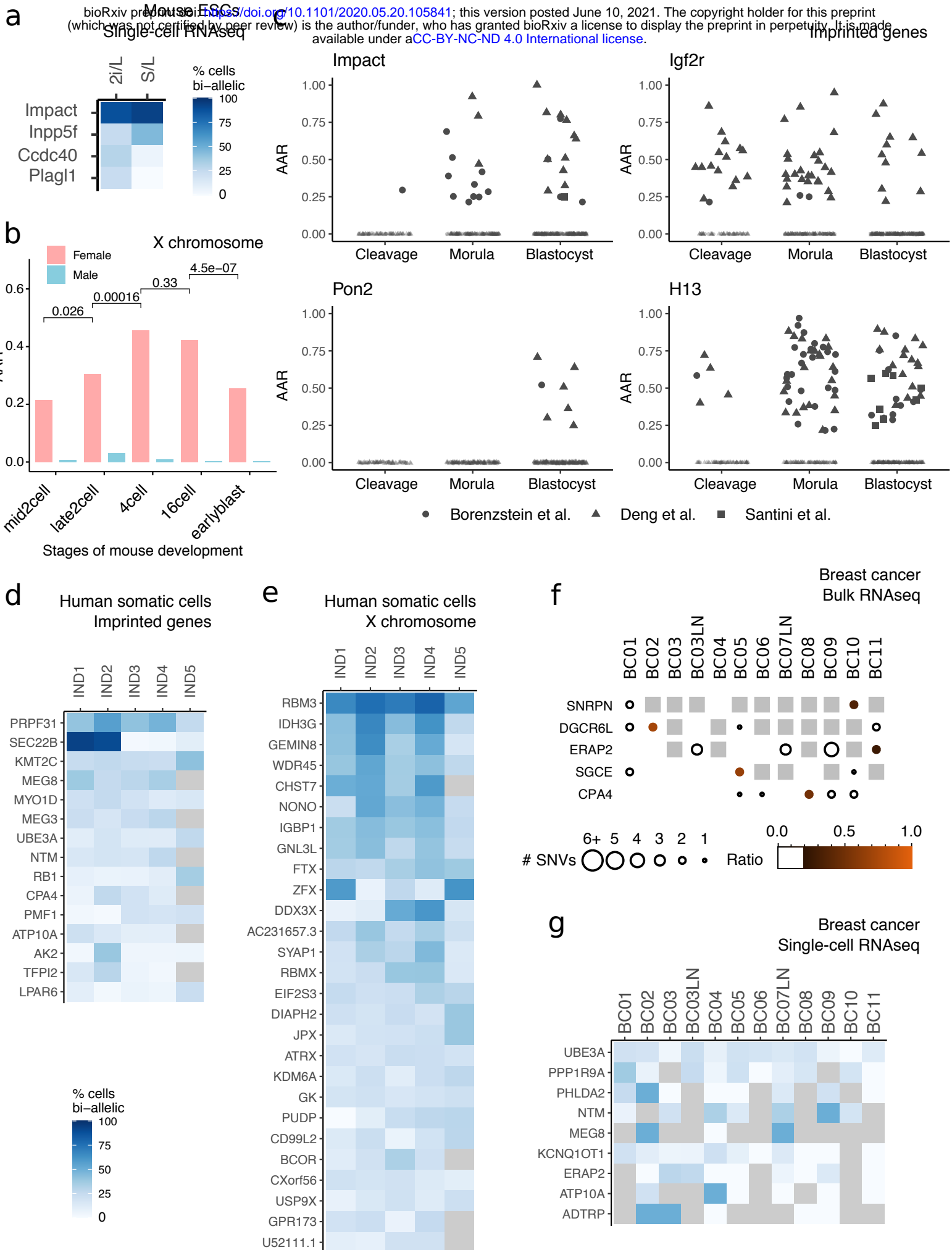
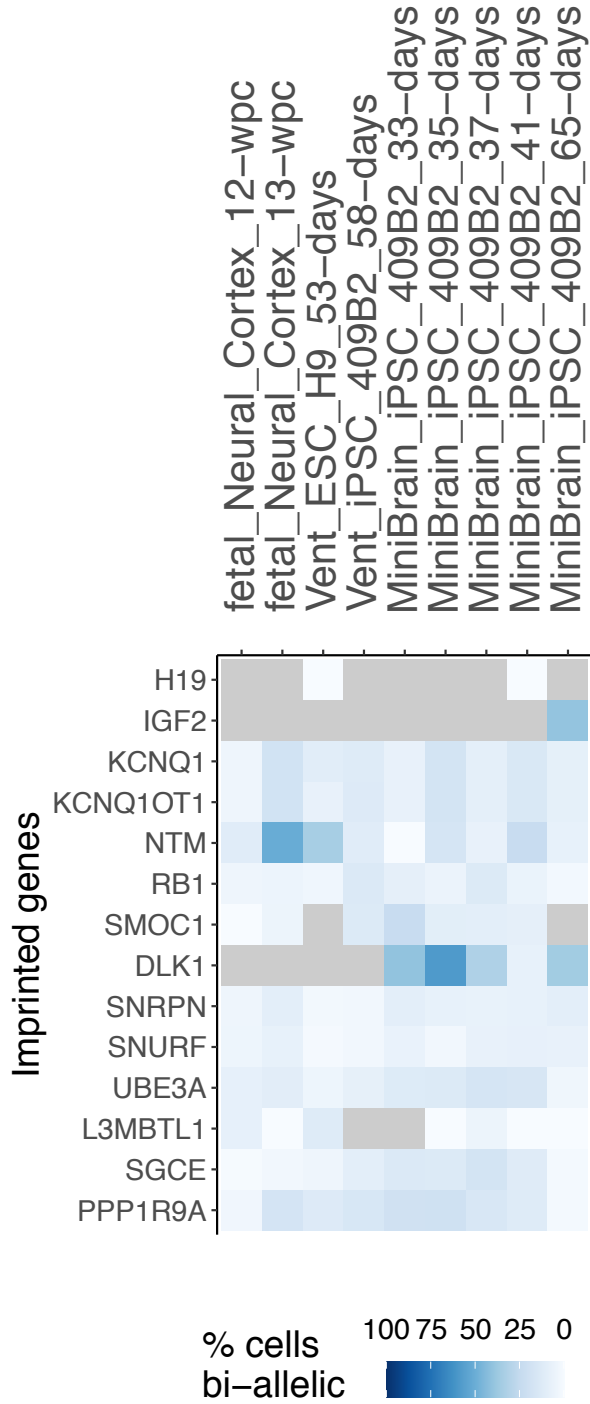


FIGURE 3

a



b

